Appl. Phys. B 66, 555–559 (1998)

Applied Physics B
Lasers
and Optics

High-energy, fourth-harmonic generation using CO_2 lasers

H.P. Chou, R.C. Slater, Y. Wang

Textron Systems Corporation, 201 Lowell Street, Wilmington, MA 01887, USA

Received: 6 July 1997/Revised version: 8 December 1997

Abstract. Fourth-harmonic conversion of a 9.55-μm CO_2 laser to 2.38 μm has been studied experimentally by using tandem $AgGaSe_2$ and $ZnGeP_2$ crystals. Up to 24 mJ per pulse of 2.38-μm radiation at a 10% overall conversion efficiency has been achieved with a mode-locked pulse format. A computer model was also developed and its predictions are in reasonable agreement with our experimental data.

PACS: 42.65 Ky

There is a great deal of interest in eyesafe laser radar. The eyesafe wavelength range extends from about 1.5 to 2.6 μm where the maximum permissible laser fluence exposure (MPE) to the human eye is about 0.1–1 J/cm^2 [1]. This is about five orders of magnitude greater than the MPE at 1.06 μm and about one to two orders of magnitude greater than the 10-μm MPE [1]. Portions of the eyesafe wavelength range (e.g., 1.52 to 1.72 μm and 2.08 to 2.44 μm) also coincide, fortuitously, with the earth's atmospheric transmission windows, allowing efficient laser propagation over many-kilometer air paths [2]. Fixed-wavelength laser radars are being considered for ranging and imaging remote objects [3]. Imaging remote objects can be accomplished by using a mode-locked laser temporal format. In this report, we describe a mode-locked 2.38-μm source generated by two-step harmonic conversion of a CO_2 laser that could be used for these applications. By comparison, it is well known that the HF laser wavelength emitting at 2.7 to 3.5 μm is strongly absorbed in the atmosphere and cannot propagate any useful distance.

Previous reports [4, 5] have shown that efficient second- and fourth-harmonic conversion of CO_2 lasers can be achieved using a mode-locked transverse excitation, atmospheric pressure (TEA) laser. The high efficiency is due in part to the short-pulse, high-intensity format available from a mode-locked source. Mode-locked temporal pulsewidths in the range 1.5–2 ns are typically produced, given the available gain bandwidth in a TEA CO_2 laser. In [4], the output from an actively mode-locked CO_2 laser was converted to 5 μm by second-harmonic generation (SHG) using an $AgGaSe_2$ (AGS) crystal, whereas in [5], it was shown that tandem $ZnGeP_2$ (ZGP) crystals were used to convert a passively mode-locked CO_2 laser to 2.4 μm in two SHG steps (9.5 μm to 4.75 μm to 2.38 μm). Although high efficiency was achieved in both cases, the relatively low laser damage threshold ($\simeq 2$ J/cm^2) still limits the reliability and performance of these devices. In a tandem crystal arrangement for generating 2.38-μm radiation, the damage is most likely to occur at the first crystal where the incident energy is greatest and high efficiency is still required. In the present paper, we demonstrate a tandem AGS/ZGP mixed-crystal arrangement to optimize the generation of CO_2 fourth-harmonic light by two-step SHG. AGS was chosen as the medium for the first SHG step because of its very low 9.55-μm absorption as compared with that of ZGP. The output energy of the first SHG step is maximized, rather than the conversion efficiency, by employing as large an incident beam radius as would fit within the first crystal cross section. This results in negligible damage to the first crystal at the expense of a modest reduction in efficiency. To date, thousands of laser shots have been put on both crystals.

The two-step SHG generation of 2.38-μm light was modeled using known properties of both crystals. The model calculations are shown to be in reasonable agreement with the experimental data.

1 Experiment

A schematic layout of the two-step SHG source is shown in Fig. 1. A repetitively pulsed CO_2 TEA laser [6] was modified for the harmonic conversion studies reported here. A master oscillator power amplifier (MOPA) configuration was integrated into the large gain volume (4 cm × 4 cm × 134 cm) of the CO_2 laser discharge described in [6]. The master oscillator (MO) and power amplifier (PA) gain volumes were roughly equal to 0.13 l. A plano–concave stable cavity was formed from a 134-cm section of gain length with 6 m of total cavity length bounded at one end by a 100 lines/mm grating mounted in a Littrow configuration for 9.55-μm oscillation. To insure lowest-order transverse-mode oscillation,

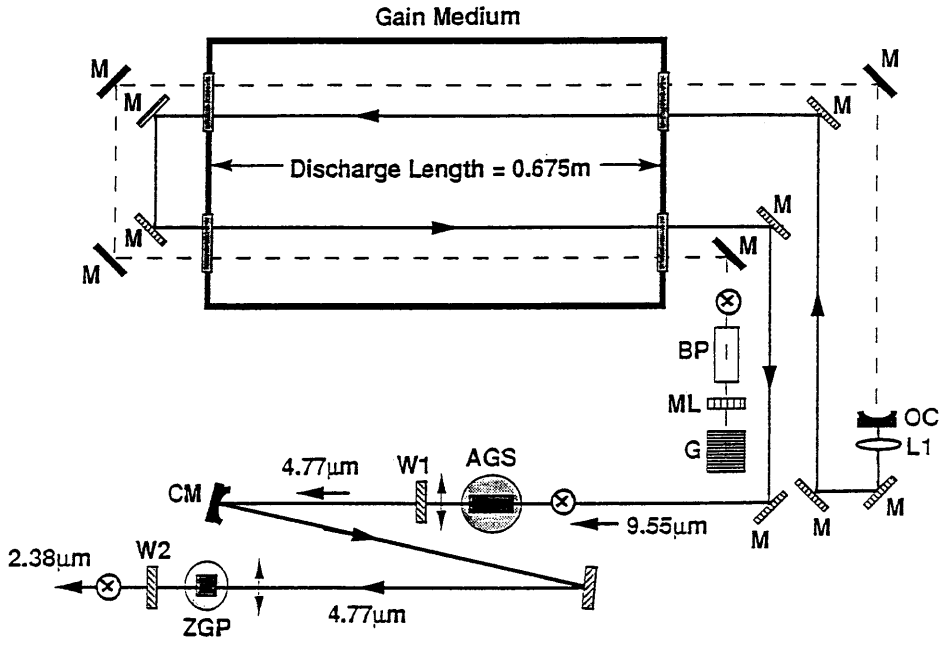

Fig. 1. Schematic diagram of CO_2-pumped two-step SHG source; *dashed line*, oscillator path; *solid line*, amplifier path. M, mirror; OC, output coupler (20% R, 10 m ROC); L1, lens (2.5 m f); BP, ZnSe Brewster plate; ML, mode locker; G, grating; AGS, NLO crystal; CM, mirror (5 m ROC); ZGP, NLO crystal; W1, AR-coated sapphire window; W2, Schott filter

an iris with diameter 1.0–1.1 cm was placed near the grating. The other end of the oscillator was an 80% output coupler with a radius of curvature of 10 m. TEM_{00} output was obtained from the MO with beam radii of 0.61 cm at the output coupler and 0.38 cm at the grating. A Spiricon Pyrocam with a 120×120 element pyroelectric array ($\approx$ 100-μm-square pixel size) was used to measure Gaussian spatial beam profiles at various points along the optical path. The cavity was actively mode-locked with a germanium standing wave acousto-optic modulator driven at 12.5 MHz yielding micropulses every 40 ns. The details of this technique are described in [7]. Individual mode-locked micropulse temporal widths were measured to be in the range of 1.5 to 2.2 ns using a 0.5-ns risetime photoelectromagnetic (PEM) detector and a high-bandwidth digitizing oscilloscope (1.0 GHz analog bandwidth, 4 GHz sampling rate). The envelope of the macropulse mode-locked train was detected with the same system. By using a calibrated calorimeter, the energy content of the MO mode-locked pulsetrain was measured to be in the range 80 to 200 mJ/macropulse depending on the discharge voltage. The MO output was recollimated and was amplified up to 600 mJ/macropulse in a single-pass PA (≈ 1 cm $\times$ 1 cm $\times$ 134 cm).

The desired 2.38-μm light was generated by fourth-harmonic conversion of the CO_2 light in two separate SHG steps. Second-harmonic generation of 9.55 μm was obtained in an anti-reflection (AR) coated, 1 cm $\times$ 1 cm $\times$ 4 cm AGS crystal cut for critically phase-matched (CPM) operation. The AR coating was designed for both fundamental and harmonic wavelengths. The AGS crystal was located in the Rayleigh range ($\approx$ 9 cm) of a 2.5-m focal length lens. An AR-coated sapphire window (transmission > 0.95) was placed at the output of the AGS crystal to separate the first-harmonic light from the fundamental. The 4.78-μm output was then converted to the desired wavelength by CPM-SHG in an AR-coated (4.78/2.38 μm) 1 cm $\times$ 1 cm $\times$ 1 cm ZGP crystal. The ZGP crystal was nominally cut at 50° for frequency doubling the 4.78-μm light. The correct phase-matching angle was determined to be 49.15° (internal) in reasonable agreement with the calculated value using recent index of refraction data [8]. The ZGP crystal was located in the Rayleigh range ($\approx$ 15 cm) of a lens with a 5-m focal length yielding a 0.3-cm beam radius. A bandpass filter (Schott RG 780, bandpass $\approx$ 0.78–2.75 μm, transmission $= 0.85$) was used to separate the 2.38-μm light from the other wavelengths.

Output energy and conversion efficiency were obtained for both SHG processes. Typical 4.78-μm energy output is plotted in Fig. 2. Two Gaussian beam radii (label "a" in Fig. 2) were used for the first SHG step (0.31 and 0.47 cm) as measured by the pyroelectric array at the input to the AGS crystal. The smaller beam size yields higher efficiency at the risk of potential damage to the AGS crystal. At the highest input energy used, the laser fluence is at the damage limit for the coated crystal (damage limit indicated by open squares in Fig. 2). At the larger beam size, the pump light just fills the crystal cross section. The conversion efficiency

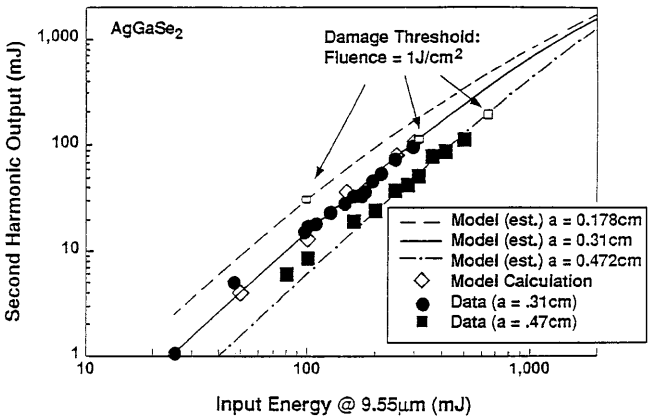

Fig. 2. First-step SHG data and model comparison. Experimental results, *solid squares* and *circles*; model calculation with spatial/temporal integration, *open diamonds*; model calculation with I_{ave}, *solid*, *dashed*, *dot/dashed lines*

is modestly reduced from > 30% to about 25%, but, more importantly, the fluence is reduced to 80% of the damage limit. We can routinely put thousands of shots at a repetition rate of 1–2 Hz onto the crystal with no damage and generate over 100 mJ/macropulse output. The 2.38-μm output energy is plotted (solid circles) in Fig. 3 using a 0.3-cm beam at the ZGP crystal and a 0.47-cm beam radius at the AGS crystal. As much as 24 mJ was generated with an overall efficiency of fourth-harmonic conversion of about 10% of the fundamental output energy. This output was obtained with about 62 mJ of 4.78-μm input energy; at this point, we began to observe signs of plasma breakdown at the AR-coated surface of the ZGP crystal and, therefore, higher energies were not investigated. The 4.78-μm fluence at breakdown was estimated to be about 0.8 J/cm^2. Preliminary data (crosses) were obtained at higher input light levels (up to 90 mJ) using an uncoated ZGP crystal. In Sect. 2, we use a model to predict the maximum fourth-harmonic output achievable with improved AR-coated ZGP crystals.

The major contribution to both conversion processes occurs within the high-intensity gain-switched spike of the TEA laser output. Temporal waveforms of the pump (see Fig. 4a) and the two converted wavelengths (see Figs 4b,c) were measured to investigate the effects of the time-varying instantaneous intensity indicative of a TEA laser macropulse. As shown in Fig. 4, the nonlinear nature of the SHG processes diminishes the amplitude of the N_2 tail in the macropulse envelope and compresses the shape of the gain-switched spike as the wavelength decreases. The fundamental contains 33% of the pulse energy in the long tail compared to 17% at 4.78 μm and virtually no energy at 2.38 μm. The full width at half maximum of the gain-switched spike lasts only 280 ns at 2.38 μm compared to 390 ns at the fundamental.

The effect of varying the micropulse intensity on the SHG conversion efficiency was obtained by decreasing the rf drive power to the AO modulator, a change which increases the micropulse temporal width. The conversion from 4.77 μm to 2.38 μm was monitored as the micropulse width varied from 1.6 to 2.5 ns. The energy output at 4.78 μm was held constant during these tests. The data shown in Fig. 5 indicate a decrease in efficiency from 30% to 18% as the pulsewidth increases. An additional data point, obtained by turning off the modelocker, yielded only a few percent efficiency. These results clearly show the improvement in 2.38-μm output that is provided by the mode-locked format.

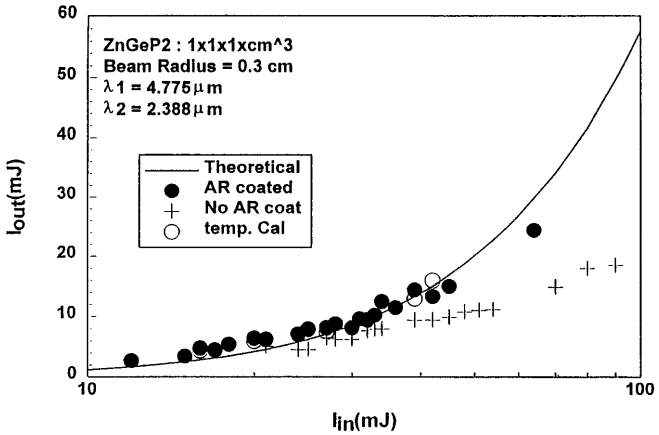

Fig. 3. Second-step SHG data and model comparison. Experimental results, *solid circles* and *crosses*; model calculation with spatial/temporal integration, *open circles*; model calculation with I_{ave}, *solid line*

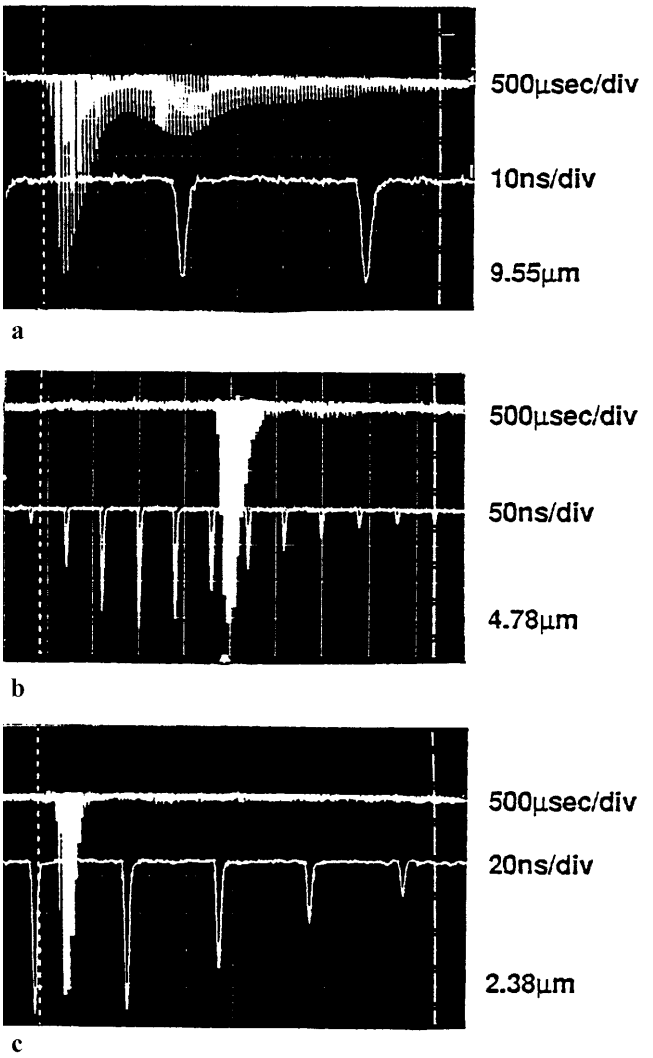

Fig. 4a–c. Single macropulse temporal records of fundamental (**a**), first-harmonic (**b**), and second-harmonic (**c**)

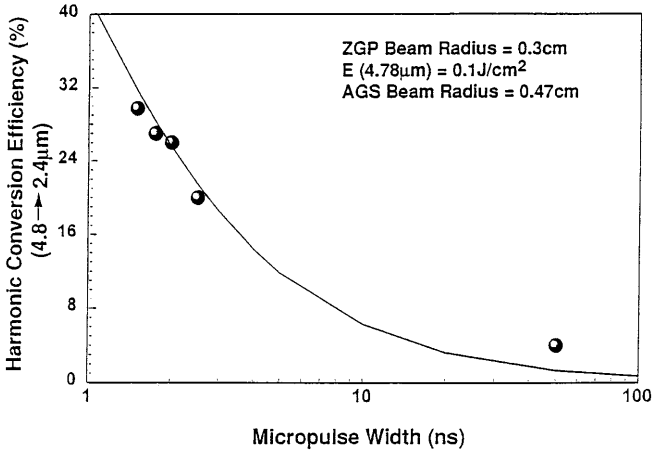

Fig. 5. Variation of 2.4-μm output as a function of micropulse temporal width

2 Model and discussion

The equations for second-harmonic generation were numerically solved to model the results in Figs. 2 and 3. We used the planewave Maxwell equations for SHG from [9] which neglect diffraction, walkoff, and dispersive effects. The maximum walkoff distance for each crystal was calculated to be 0.27 cm in AGS and 0.07 cm in ZGP, both lengths small compared to the measured beam diameters. The model inputs which describe the appropriate crystal properties for SHG are listed in Table 1. All the numerical values used in Table 1 come from [8], except for the indices of refraction for AGS, which come from [10] and the ZGP absorption which comes from [11].

For quantitative comparison of the model and experiment, the space and time variation of the input electric field strength needs to be evaluated for each SHG step. The Gaussian spatial dependence of the pump beam is included explicitly for each SHG step using measured beam radii at each crystal. As shown in Fig. 4, the temporal form of the CO_2 laser output is made up of a gain-switched spike and long-time N_2 tail. We performed an explicit temporal integration for both SHG conversion steps by approximating the temporal waveform as follows. The macropulse envelope was approximated by two triangular functions of differing heights and bases (one for the gain-switched spike and one for the long-time tail), and the micropulses were approximated by rectangles with a temporal width equal to the measured full width at half maximum (FWHM) of each micropulse. The results for each SHG step are shown as the open diamonds and circles, respectively, in Figs. 2 and 3 only for the case where the beam radius at the AGS crystal was 0.47 cm. The model predictions are in reasonable agreement with the measured output energies over the input laser energy range used.

After performing these detailed calculations, we found that the temporal integration could be simplified by ignoring the long-time tail contribution and approximating the pulsetrain in the gain-switched spike as a series of equal-amplitude rectangular micropulses with an intensity of $\sim 70\%$ of the intensity of the peak amplitude micropulse. These approximate results are shown as continuous lines in Figs. 2 and 3. The error is about 5%–8% relative to the more detailed model calculation. We have also included in our model calculations a prediction for one of the beam sizes (radius $= 0.178$ cm) used in [4] assuming a temporal waveform as was obtained with our laser. It is evident from these data that the use of a large beam radius at the first crystal was advantageous in fourth-harmonic generation.

The fourth-harmonic conversion output energy and efficiency could be improved beyond what has already been measured if lower absorption, longer ZGP crystals with a higher damage threshold were used [12]. The absorption of our current 1-cm-long ZGP crystal is shown in Table 1. Using our model, we estimate that the energy output in Fig. 3 could be further increased by $> 100\%$ (up to 58 mJ) using the highest available 4.78-μm output (≈ 100 mJ). In addition, using longer crystal lengths of up to 2.5 cm with low absorption ($< 0.05\,\mathrm{cm}^{-1}$) at 4.78 μm and 2.38 μm, we calculate that fourth-harmonic output in the range of 90 mJ would be the maximum obtainable from a source of the type shown in Fig. 1. This maximum value is due to limitations on crystal length, fluence damage requirements, absorption and temporal micropulse widths based on the TEA laser gain bandwidth. More trade studies need to be done to improve the output energy.

Our use of an AGS crystal as the first-harmonic converter medium will allow wavelength tunability over a range of CO_2 laser lines especially during repetitively pulsed operation. AGS optical absorption is quite weak in the 5–10 μm region. Fourth-harmonic conversion should then be possible over a number of J lines in both P and R branches of the 9.6 μm and 10.6 μm bands. By contrast, the use of ZGP as the first converter would severely limit efficient tunability because of strong 10-μm absorption and associated thermal lensing.

It should be noted that potential use of this type of device as a laser radar would require CO_2 laser operation at the P(18) rather than the P(20) line used in these laboratory tests of laser performance. High-resolution atmospheric transmission measurements indicate that the P(18) line falls within a narrow transmission window (for example, 70% transmission over a 5-km horizontal path at sea level) whereas the P(20) and P(22) lines fall accidentally on molecular absorption lines. Performance of the fourth-harmonic conversion at this wavelength should be nearly identical (within a few percent) to the reported performance at P(20) described in this report.

In summary, we have shown that a mode-locked MOPA CO_2 TEA laser system pumping a series arrangement of AGS and ZGP nonlinear crystals is a source of at least 24 mJ of 2.38-μm light. Although average power issues were not undertaken in these studies, this output level was observed to be maintained at a 1–2-Hz pulse rate.

Table 1. Crystal parameters for model

$AgGaSe_2$ Crystal (uniaxial negative)	$ZnGeP_2$ (uniaxial positive)
ordinary index at 9.55 μm $= 2.5969$	extraordinary index at 4.78 μm $= 3.1389$
extraordinary index at 4.78 μm $= 2.583$	ordinary index at 2.38 μm $= 3.15547$
Type I PM O+O–E	Type I PM E+E–O
$d_{36} = 3.3 \pm 0.3 \times 10^{-11}$ m/V	$d_{36} = 8.54 \pm 1.3 \times 10^{-11}$ m/V
phase match angle $= \theta_m = 49°$	$\theta_m = 49.15°$
$d_{\mathrm{eff}} = d_{36} sin(\theta_{\mathrm{m}})$	$d_{\mathrm{eff}} = d_{36} sin(2\theta_{\mathrm{m}})$
absorption coefficient (9.55 μm) $< 0.02\,\mathrm{cm}^{-1}$	absorption coefficient (4.775 μm) $< 0.055\,\mathrm{cm}^{-1}$
absorption coefficient (4.78 μm) $< 0.02\,\mathrm{cm}^{-1}$	absorption coefficient (2.38 μm) $= 0.55\,\mathrm{cm}^{-1}$

Acknowledgements. We thank Dr. Richard Eng (TSC) for several fruitful discussions. The continuing support of the Air Force Phillips Laboratory under Contract F29601-95-C-0223 is gratefully acknowledged. We would also like to thank Steve Caracci (Wright Patterson Air Force Base) for loaning us the ZGP crystals.

References

1. ANSI Standard for the Safe Use of Lasers, (American National Standards Institute, New York 1993) ANSI Z136.1
2. A.J. LaRocca: In *The Infrared Handbook*, ed. by W.L. Wolfe, G.J. Zissis, (Environmental Research Institute of Michigan, Ann Arbor, MI 1978) Chap. 5

3. D.G. Youmans, F. Corbett, G. Dryden, M. Kovacs: Proc. Soc. Photo-Opt. Eng. **2702**, 40 (1996)
4. M.W. McGeoch: Proc. SPIE **1871**, 62 (1993)
5. Y. Andreev, V. Baranov, V. Voevodin, P. Geiko, A. Gribenyukov, S. Izyumov, S. Kozochkin, V. Pis'mennyi, Y. Satov, A. Strel'tsov: Sov. J. Quantum Electron. **17**, 1435 (1987); for non-modelocked fourth-harmonic generation see also Yu.M. Andreev, T.V. Vedernikova, A.A. Betin, et.al.: Sov. J. Quantum Electron. **15**, 1014 (1985)
6. S. Ghoshroy, H.P. Chou, Y. Wang, F. Faria-E-Maia, S. Kurzius: Proc. 3rd International DRA/NASA Conf. on Long-life CO_2 Laser Technology, Malvern, UK (1992) p. 13
7. H. Chou, R. Eng, V. Hasson, F. Faria-E-Maia, Y. Wang: Conf. on Gas and Chemical Lasers, San Jose, CA, Proc. SPIE **2702**, 106 (1996)
8. V.G. Dmitriev, G.G. Gurzadyan, D.N. Nikogosyan: *Handbook of Nonlinear Optical Crystals* (Springer, Berlin, Heidelberg 1990)
9. D. Neuschafer, Hp. Preiserk, H. Spahni, E. Konz, G. Marowsky: J. Opt. Soc. Am. B **11**, 649 (1994)
10. D.A. Roberts: Appl. Opt. **35**, 4677 (1996)
11. J.H. Churnside, J.J. Wilson, A. Gribenyukov, S. Shubin, S. Dolgi, Y. Andreev, V. Zuev: Frequency Conversion of a CO_2 Laser with $ZnGeP_2$, NOAA Technical Memorandum ERL WPL-224, Wave Propagation Laboratory, Boulder, CO (July 1992)
12. The ZGP coating vendor (Inrad, Northvale, NJ) claims a relative improvement in the coating damage threshold above what has been reported here. The vendor reports absorption of $0.05\,\mathrm{cm}^{-1}$ at $2.38\,\mu\mathrm{m}$ and $< 0.05\,\mathrm{cm}^{-1}$ at $4.77\,\mu\mathrm{m}$ for ZGP crystals up to 25 mm in length